RSC Advances

ROYAL SOCIETY OF CHEMISTRY

www.rsc.org/advances

Journal Name

ARTICLE

Electrochemical probing of carbon quantum dots: not suitable for a single electrode material

Received 00th January 20xx,
Accepted 00th January 20xx

DOI: 10.1039/x0xx00000x

www.rsc.org/

Xinnan Jia and Xiaobo Ji*

In this article graphene quantum dots (GQDs) were prepared from activated graphene oxide (AGO) for the first time utilizing a reflux route. We focus on the relationship between surface structure and electrochemical activity of graphene oxide (GO), AGO, GQDs and reduced graphene quantum dots (RGQDs). Surprisingly it was found that GQDs exhibited much slower electron transfer rate of 1.105×10^{-4} cm s^{-1} compared with GO of 1.918×10^{-3} cm s^{-1} and AGO of 6.316×10^{-3} cm s^{-1}. Obviously, GQDs modified electrode surface can be completely blocked which might result from its low edge-to-basal plane rate though easy aggregation, rapid stacking and high oxygen-functional groups. Contrary to a general view that size-reducing is favorable to electrochemical kinetics, such findings, never reported before, imply that GQDs may not be suitable for applying for a beneficial single electrode material. GQDs, a new type of advanced materials of nanoscale, must be applied in a proper way in order to exert potential superiority to an utmost extend.

Introduction

Graphene-based materials have attracted ongoing enthusiasm in recent years as electrochemical materials in energy storage devices such as its reported use in supercapacitors and batteries. With the advent of nanotechnology, extensive efforts have been focusing on converting graphene to 0 D graphene quantum dots (GQDs) which are graphene sheets in the range of a few nm to ~100 nm[1]. Owing to the quantum confinement and edge effect[2, 3], GQDs can be simply modified through controlling the size and present many unique properties including high surface area, fine dispersion in water solvents, strong luminescence, low toxicity and excellent biocompatibility [4, 5]. Consequently, these dots are proposed to be applicable as the composite electrode materials to enhance electrochemical performances in Li or Na ion batteries and supercapacitors[6-9]. Chao et al. has elegantly shown that GQDs are successfully coated onto the VO_2 surfaces, which demonstrated high Na storage capacity of 306 mAh/g at 100 mA/g , good rate properties and superior cycling life[9]. GQDs have also been reported to exhibit enhanced properties towards the devices of bioimaging[10], sensors[11], catalysis[12] and photovoltaic[13].

While many optimistic reports of utilizing GQDs have emerged, it is shown that GQDs may not provide an excellent advantage as single electrode materials. Zhu et al. has clearly indicated that the specific capacitance of GQDs is found to reach at only 53 F g^{-1}, where GQDs are employed as the single electrode materials[6], exhibiting a lower capacitance compare to other carbon materials, such as graphene[14] of 104.4 F g^{-1}, and mesoporous carbon[15] of 200 F g^{-1}.

Note that in previous studies, two key methods have been explored to obtain GQDs, one of which is directly cutting graphite crystallites or graphene oxide sheets into 0D GQDs via electron beam lithography[16], hydrothermal or solvothermal technique[17], electrochemical route[18] and ultrasonic method[19]. Another strategy for synthesizing GQDs is in chemical way though pyrolyzing suitable organic precursors or catalyzing fullerene on the surface of ruthenium into small fragments[20-22]. However, the extremely tedious process, violent reaction conditions, low yield and long time of these methods limit their application in electrochemical field.

Herein, we report an optimized methodology to obtain GQDs by chemically cutting an ordinarily utilizing flake graphite. After exfoliating the graphite with Hummers method[23], we utilize activated graphene oxide (AGO) rather than graphene oxide (GO) to prepare the final product, which should shorten the reaction time or lower the temperature compared with the previous reported methods. Then we compare the effect of coverage when utilizing GO, AGO, GQDs and reduced graphene quantum dots (RGQDs) respectively as electrode materials for 1 mM potassium ferrocyanide in 0.1 M KCl. Most interestingly, we demonstrate for the first time that GQDs exhibit slow heterogeneous electron transfer (1.105×10^{-4} cm s^{-1}), mainly attributed to easy aggregation, rapid stacking and high oxygen-functional groups at the edges of GQDs. Considering that GQDs, the mini graphene sheets, are similar to graphene that the edge plane contributes to accelerate the electron transfer rather than basal plane[24, 25]. The disadvantages mentioned above lead to low edge-to-basal plane ratio and consequently GQDs appear to be an inferior single electrode material. Nevertheless, GQDs are promising

Department of Chemistry and Chemical Engineering, Central South University, Changsha, 410083, China. E-mail: xji.csu.edu@gmail.com; Fax: +86-731-88879616; Tel: +86-731-88879616

building blocks for future electrochemical nanomaterials applied for the surfactant, as well as composites with other materials, where the former aim to control structure and the latter to inhibit irreversible process and improve cycling stability. In this perspective, more professional work should be performed to further realize mass production so as to develop the applications of GQDs.

Experimental section

Materials Synthesis

Preparation of GO and AGO. GO was prepared from flake graphite by the modification of Hummers method as reported earlier[23, 26]. 200 mg of GO solid was dispersed in water (twice-distilled water with a resistance not less than 18 MΩ was used) by ultrasonication. 1.3 g of KOH (the ratio of KOH/GO was controlled in 6.5) was dispersed in water at the same time. Then, the two kinds of aqueous solution were mixed together with magnetic stirring for 5 h. The obtained solution was dried at 55 ℃. The dried GO/KOH mixture was further annealed in a quartz tube furnace under Ar atmosphere at 800 ℃ for 30 min to produce AGO. Finally, the AGO was obtained after being washed several times with diluted HCl and deionized water in sequence to remove the residual alkali completely, followed by drying at 80 ℃.

Preparation of GQDs and RGQDs. In a modification method, 400 mg of AGO was dispersed in 150 mL of HNO_3 (12 mol L^{-1}) aqueous solution in 500 mL volumetric flask and sonicated (100 W, 40 kHz) for 2h. Then the mixture was refluxed at 100 ℃ for 48 h. After cooling to room temperature, the suspension was filtered through a microporous membrane filter to remove the sediment. Subsequently, the filtrate was heated to evaporate HNO_3 and a part of water. The final solution was further dialyzed for 48 h to remove impurities in a dialysis bag and then dried in an oven at 55 ℃ for 12 h to obtain the GQDs powder.

RGQDs were prepared through hydrothermal reduction treatment using hydrazine hydrate, because it hardly changed the morphology of substance. Briefly, 30 mg of GQDs were dispersed in deionized water by ultrasonication. Then 2 mL of hydrazine hydrate was added into solution when the solution was heated at 98 ℃. The mixed solution was refluxed at 100 ℃ for 24 h and cooled down to room temperature to form RGQDs.

Material characterization

Transmission electron microscopy (TEM) was obtained by using a JEM-2100F transmission electron microscope. The elemental composition was analyzed with an X-ray photoelectron spectroscopy (XPS, ESCALab250) in order to determine oxygen content of materials. UV-vis absorption spectra (Abs) were collected on a UV-vis spectrophotometer (UV-1801). Photoluminescence (PL) spectra were conducted using a fluorescence spectrophotometer (F-4600).

Electrochemical measurements

All the measurements were performed with a three electrode system. A glassy carbon (GC) electrode as a working electrode was prepared for modification by renewing the electrode surface. It was polished with 0.05 mm alumina particles on a cloth and ultrasonicated in ethanol and water for 5 min. This was repeated several times. Then the aliquots of carbon materials dispersed in ethanol (0.4 mg per 1 mL) were carefully pipetted onto the GC electrode surface using a micro-pipette. The solvent was allowed to volatilize at room temperature, when a randomly distributed film is left on the GC electrode surface. A platinum electrode served as a counter electrode, while a Hg/HgCl electrode served as a reference electrode. Cyclic voltammetry (CV) experiments were collected on a Modulab (Solartron Analytical) electrochemical workstation by using KCl (0.1 M) as supporting electrolyte for potassium ferricyanide (1 mM).

Results and discussion

The chemical process of GQDs was illustrated in Scheme 1. GO was obtained according to Hummers method. After KOH activation of GO, AGO was prepared with luxuriant pore structure and further cut into mini size GQDs through refluxed by HNO_3. Finally, GQDs were reduced by hydrazine hydrate while retaining its morphology. The digital images of GO, AGO, GQDs and RGQDs were displayed respectively in Fig. 1a, 1b, 1c and 1d. It was clear that GO turned from red-brown flake into black powder after activation. GQDs, dark brown powder, became black powder after reduction. As could be seen from the digital image of Fig. 1e, AGO and RGQDs were insoluble in aqueous solution while GO was well dispersed in water solution treated by sonication and GQDs were water-soluble without ultrasonic dispersion resulting from different oxygen contents on the surface according to XPS test below. Particularly, GQDs aqueous solution could be conserved more than 6 months without aggregation at room temperature. Fig. 2a showed TEM images of the GO films. Dense 3D pore structure and predominantly atom-thick wall were further confirmed by the TEM of AGO (Fig. 2b and c). In addition, as could be shown in the TEM of GQDs (Fig. 2d and e), the diameters of the GQDs appeared to be in the range of 8-10 nm. Note that the chemical activation with KOH had been widely used to obtain AGO with high specific surface areas (SSA) and

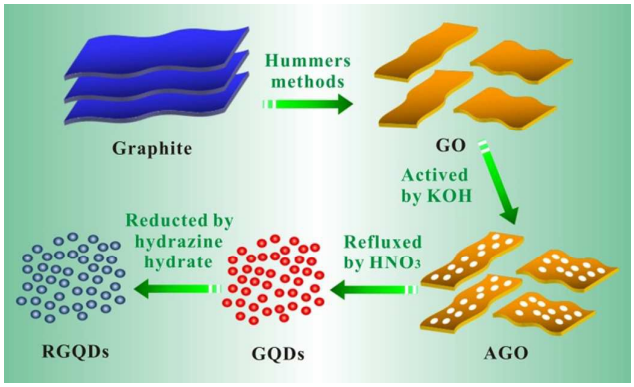

Scheme 1 Schematic illustration of the synthesis process of the GQDs

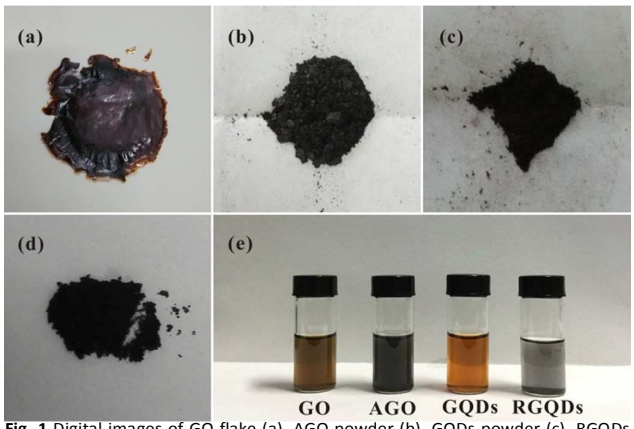

Fig. 1 Digital images of GO flake (a), AGO powder (b), GQDs powder (c), RGQDs powder (d) and their aqueous solutions (e).

dense three dimensional pore structure[27]. Therefore, the smaller GO fragments and more pore defects generated in reaction contribute to produce GQDs in gentler reaction conditions than large-thick GO flake and graphite. The activation process using KOH was explained in general as follows[28]:

$$6KOH + 2C \rightarrow 2K + 3H_2 + 2K_2CO_3$$

The formation of the GQDs was further confirmed by the optical properties in Fig. 3a. It showed a broad UV-vis absorption from 800 nm to 200 nm with one shoulder around 490 nm and one peak at 214 nm owning to the $\pi \rightarrow \pi^*$ transition of aromatic sp^2 domains[29], which was also observed in GQDs synthesized by chemical oxidation and hydrothermal methods[17, 30]. As we could see in the picture, the solution of GQDs emitted strong yellow photoluminescence (PL) under excitation at 365 nm. In addition, the PL spectrum was generally broad and depended on excitation wavelength called excitation-dependent PL behavior. When the excitation wavelength increased from 420 nm to 520 nm, the PL peaks exhibited a red-shift from 520 nm to 580 nm with the remarkable decrease of its intensity and the strongest PL intensity appears under excitation at 460 nm. This phenomenon may ascribe to optical selection by different sizes[31], different emissive sites and surface defects of GQDs,

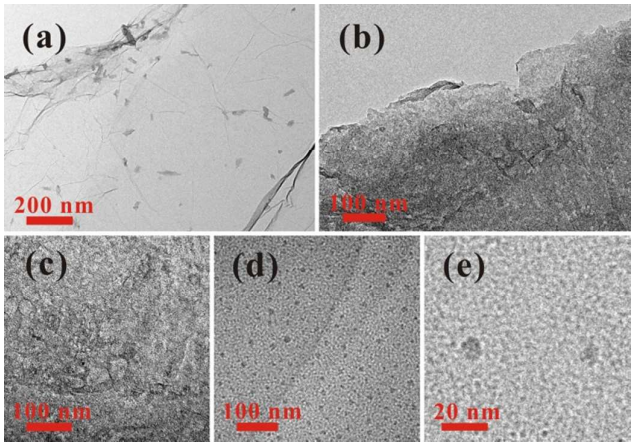

Fig 2 TEM images of GO (a), AGO (b and c) and GQDs with different magnifications (d and e).

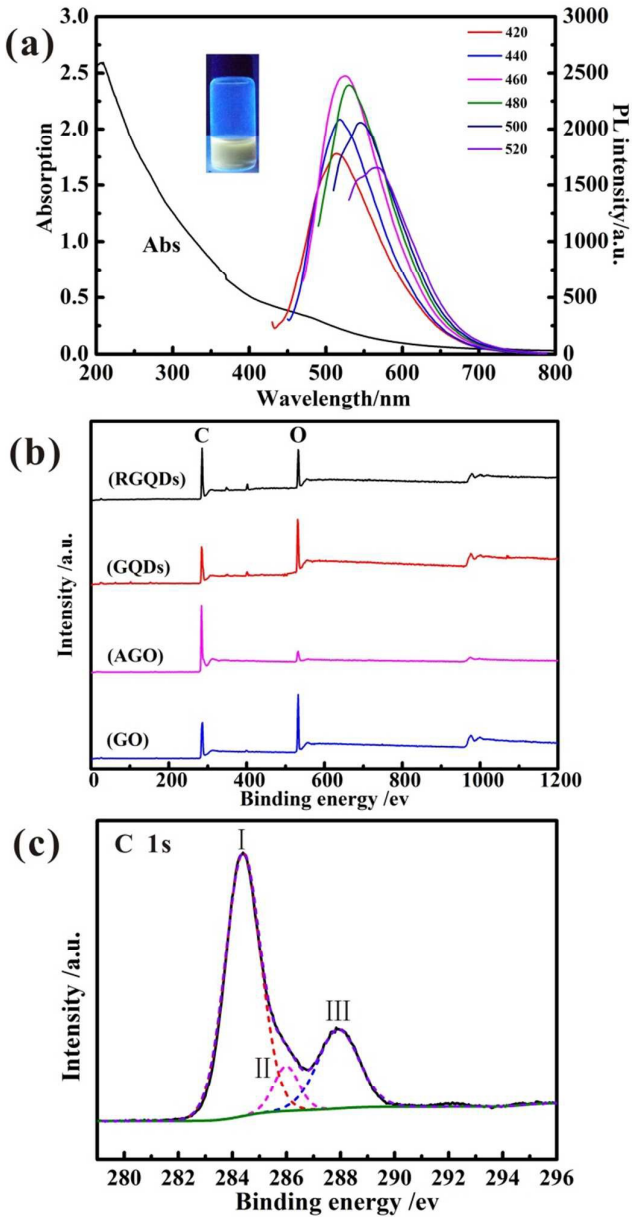

Fig. 3 UV-vis absoption and PL emission spectra of GQDs in aqueous solution (a). (Inset: Optical photograph of GQDs solution under UV beam of 365 nm). XPS spectra of GO, AGO, GQDs and RGQDs (b). C 1s core level XPS spectra of GQDs (c).

similarly to the excitation-dependent PL of other luminescent carbon-based nanomaterials[32].

The X-ray photoelectron spectra (XPS) was conducted to analysis oxygen content of GO, AGO, GQDs and RGQDs and the C/O ratios were calculated based on C 1s and O 1s intensities. The X-ray photoelectron spectroscopy spectra records were shown in Fig. 3b, and the corresponding C and O atom ratios were listed in Table 1. The oxygen content of GQDs was the highest than the other carbon materials, on account of its edge effects[3] that can increase more oxygen functional groups during the chemical oxygen process, while the AGO was the lowest one due to carbon-oxygen bond easily broken at activated temperature of 800 ℃[28]. When the GQDs was

Table 1 Calculated properties of GO, AGO, GQDs, RGQDs

Sample	GC	GO	AGO	GQDs	RGQDs
Carbon atom ratio (%)	—	67.41	91.65	61.76	72.02
Oxygen atom ratio (%)	—	30.81	8.35	34.65	23.33
E_{pa} (mv)	220	258	223	301	300
E_{pc} (mv)	142	107	126	22	25
ΔE_p (mv)	78	151	97	279	275
ψ	1.42638	0.198915	0.65501	0.01146	0.01396
k^0	1.375×10^{-2}	1.918×10^{-3}	6.316×10^{-3}	1.105×10^{-4}	1.346×10^{-4}

reduced to RGQDs, the oxygen content decreased from 34.65 %to 23.33 %. The C-1s peak of GQDs was consisted of three Gaussian peaks (Figure 3c) centered at 284.39 eV (peak I), 285.99 eV (Peak II) and 287.8 eV (Peak III), indicating a considerable degree of oxidation corresponding to carbon atoms in different functional groups, which were sp^2 carbon at ≈ 284.39 eV, C of C-O and/or C-OH bonds at ≈ 285.99 eV, C of C=O bonds at ≈ 287.8 eV[33, 34].

We next turned to investigate the electrochemical properties of a chemical modified GC electrode following modification with 4.8 μg of GO, AGO, GQDs and RGQDs using the ferro/ferricyanide redox probe for comparative purpose. The heterogeneous electron transfer (HET) property was illustrated through determination of the electron transfer rate kinetics (k^0) from cyclic voltammetric, which was evaluated using the Nicholson equation for an electrochemically quasi-reversible process as demonstrated by the equation (1)[35, 36]:

$$\Psi = k^0 [\pi DnvF/(RT)]^{-1/2} \quad (1)$$

Every symbol has their ordinary meaning, in which Ψ is a kinetic parameter without dimension, D is the diffusion coefficient for $[Fe(CN)_6]^{3-/4-}$ in 0.1 M KCl (7.6×10^{-6} cm^2s^{-1})[37], n is the number of electrons working in the electron-transfer process, v is the scan rate, R is the molar gas constant and T is the temperature. Ψ, the kinetic parameter, is fitted the function of Ψ-ΔE_p for a one electron redox reaction (α = 0.5, T = 298 K) as described by the equation (2)[35, 36]:

$$\Psi = (-0.6288 + 0.0021\,X)/(1 - 0.017\,X) \quad (2)$$

Where $X = \Delta E_p = E_{pa} - E_{pc}$, is the peak-to-peak separation in the recorded voltammetry.

Note that it was ordinary to classify the layered structure of graphite into two graphite plane: the basal plane, which existed all the side of graphite layer as well as the surface paralleling to it, and the edge plane, which was from the peripheral edge perpendicularly to the basal plane[14, 38, 39]. The two planes demonstrated significantly different actions in accelerating electron transfer due to the property of the chemical bonding. When the edge plane was overwhelmingly dominant over the basal plane, the electron transfer was much faster compared to that of being converse. Meanwhile, the oxygen functional groups draw notably attention in influencing electrochemical properties both through the electron-exchange rate and the adsorption of molecules from electrolyte in the redox reaction[40, 41].

Fig. 4 depicted the cyclic voltammograms curves and Table 1 displayed the calculation of corresponding peak-to-peak separation (ΔE_p) and k^0. It could be seen that GQDs modified electrode showed high peak separation (ΔE_p) of 279 mV at 100 mVs^{-1} resulting in the slow HET at 1.105×10^{-4} cm s^{-1}, which was similar to that observed at RGQDs (275 mV; 1.346×10^{-4} cm s^{-1}) and significantly slower than that observed at both GO modified electrode and AGO modified electrode (151 mV; 1.918×10^{-3} cm s^{-1} and 97 mV; 6.316×10^{-3} cm s^{-1} respectively). It had been reported that GO exhibited slow electron transfer due to the structural effects, where the oxygen-containing groups, low edge plane content and low specific surface area were taken into consideration.[14] The AGO reflected a fast electron transfer with great amount of pore defects and relatively low oxygen content, which were beneficial to contain a large ratio of the edge plane to the basal plane. Notably, GQDs exhibited much slower electrode kinetics than GO as if the electrode surface was completely blocked, mainly due to the increasing oxygen-containing groups leading to restrain the electron transfer between GQDs and ferro/ferricyanide. Moreover, GQDs/RGQDs were stacked irregularly in a short time as soon as the solvent evaporated, leading to decrease the specific surface area in fact. Also as Hou et al. had pointed out, the Brunauer-Emmett-Teller (BET) SSA of carbon quantum dots was only 18.6 m^2 g^{-1} calculated from nitrogen adsorption-desorption isotherms[42]. In the real experimental case the carbon-based materials were immobilized onto the GC electrode surface so that the materials were accumulated layer upon layer and the SSA of GQDs/RGQDs would likely to be smaller. As a consequence, both GQDs and RGQDs modified electrodes demonstrated effectively blocked because the basal plane substituting the edge plane became the main way to transfer electrons and it was adverse to increase the electron transfer kinetics.

Fig. 5 depicted the digital images of different amounts of GQDs and RGQDs modified GC electrode. The picture clearly conveyed the significant information that GQDs/RGQDs

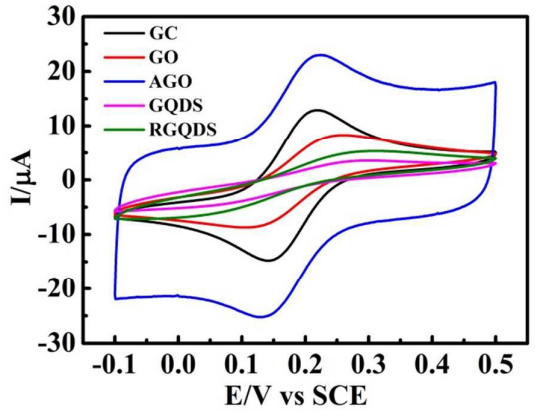

Fig. 4 Cyclic voltammetric profiles recorded of GO, AGO, GQDs and RGQDs modified GC electrode utilizing 1 mM potassium ferricyanide in 0.1 M KCl. Scan rate: 100 mVs^{-1} (*vs.* SCE)

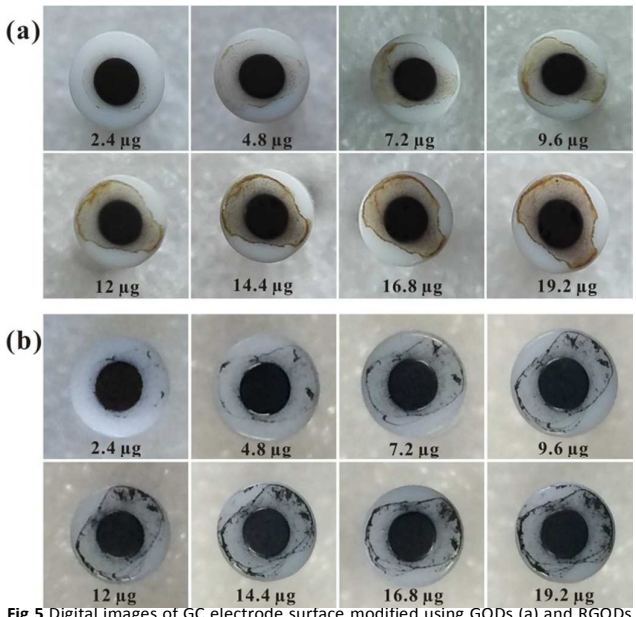

Fig 5 Digital images of GC electrode surface modified using GQDs (a) and RGQDs (b) with different amounts.

stacked heavily as increasing their mass. The effect of increasing materials' amount deposition on the GC electrode surface was also depicted in Fig. 6. It showed that with an increasing GO' mass coverage on the GC electrode (Fig 6a) the peak-to-peak separation tended to be stable, while the peak current descended apparently. This was due to the low conductivity of GO and flakes accumulation[25]. Considering the effect of increasing amounts of AGO on the voltammetric curve (shown in Fig. 6b), it was a gradually high current response and a clearly narrow shift between oxidation and reduction peak, owning to the fact that the more porous structures with high specific surface areas[14] contributed to a higher number of edge-like structures. We next turned to exploring the effect of increasing GQDs' mass. As was evident

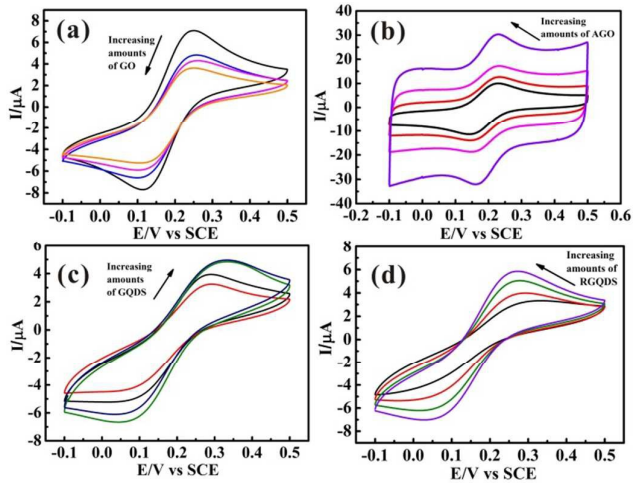

Fig. 6 Cyclic voltammetric profiles recorded utilizing 1 mM potassium ferricyanide in 0.1 M KCl, obtained using an GC electrode with the addition of increasing amounts of 2.4, 4.8, 9.6 and 16.8 μg GO (a), AGO (b), GQDs (c) and RGQDs (d). Scan rate: 50 mVs^{-1} (*vs*. SCE).

in Fig. 6c, the ΔE_p had a conspicuously large shift which was different from GO and AGO. It proved that the modified GC electrode surface with a little quantities of GQDs existed incomplete coverage site where the exposed surface remained relatively electrochemically active, thus with increased coverage of GQDs, the "uncovered active sites" disappeared gradually and consequently the heterogeneous electron transfer slowed down. At the same time, the basal plane sites of GQDs completely controlled the electrode reactivity inducing "blocking" on the electrode surface. The "blocking" was ameliorated a little to some degree as GQDs was reduced (displayed in Fig 6d), resulting from the decreasing oxygen-containing groups. The above interesting findings demonstrated that GQDs were no better than graphene for an excellent single electrode material.

Conclusions

To summarize, we have improved the strategy to prepare GQDs directly by refluxing AGO with the advantages of tender conditions. Moreover, we have compared, for the first time, the electrochemical properties of GO, AGO, GQDs and RGQDs. Interestingly, it is found that GQDs modified electrode surface is blocked, exhibiting slow heterogeneous electron transfer kinetics due to slow edge/basal plane ratio. Easy aggregation, rapid stacking and high oxygen-functional groups of GQDs have a negative impact on the electrochemical properties. Consequently, GQDs, as a single electrode material, exhibit a poor property. Whereas it still has huge potential to be surfactant or composite with other materials, if we keep turning a bright eye on it and use it in a proper way.

Acknowledgements

This work was financially supported by National Natural Science Foundation of China (21473258), Distinguished Young Scientists of Hunan Province (13JJ1004), and the Hunan Provincial Innovation Foundation for Postgraduate (CX2015B039).

Notes and references

1. X. Li, X. Wang, L. Zhang, S. Lee and H. Dai, *Science*, 2008, **319**, 1229-1232.
2. Ç. Ö. Girit, J. C. Meyer, R. Erni, M. D. Rossell, C. Kisielowski, L. Yang, C.-H. Park, M. F. Crommie, M. L. Cohen, S. G. Louie and A. Zettl, *Science*, 2009, **323**, 1705-1708.
3. K. A. Ritter and J. W. Lyding, *Nat. Mater.*, 2009, **8**, 235-242.
4. J. Shen, Y. Zhu, X. Yang and C. Li, *Chem. Commun.*, 2012, **48**, 3686-3699.
5. Z. Zhang, J. Zhang, N. Chen and L. Qu, *Energy Environ. Sci.*, 2012, **5**, 8869-8890.
6. Y. Zhu, X. Ji, C. Pan, Q. Sun, W. Song, L. Fang, Q. Chen and C. E. Banks, *Energy Environ. Sci.*, 2013, **6**, 3665-3675.

7. J. Pan, Y. Sheng, J. Zhang, J. Wei, P. Huang, X. Zhang and B. Feng, *J. Mater. Chem. A*, 2014, **2**, 18082-18086.
8. H. Ming, Y. Yan, J. Ming, X. Li, Q. Zhou, H. Huang and J. Zheng, *RSC Adv.*, 2014, **4**, 12971-12976.
9. D. Chao, C. Zhu, X. Xia, J. Liu, X. Zhang, J. Wang, P. Liang, J. Lin, H. Zhang, Z. X. Shen and H. J. Fan, *Nano Lett.*, 2015, **15**, 565-573.
10. S. Zhu, J. Zhang, C. Qiao, S. Tang, Y. Li, W. Yuan, B. Li, L. Tian, F. Liu, R. Hu, H. Gao, H. Wei, H. Zhang, H. Sun and B. Yang, *Chem. Commun.*, 2011, **47**, 6858-6860.
11. Y. Dong, G. Li, N. Zhou, R. Wang, Y. Chi and G. Chen, *Anal. Chem.*, 2012, **84**, 8378-8382.
12. X. Zhou, Z. Tian, J. Li, H. Ruan, Y. Ma, Z. Yang and Y. Qu, *Nanoscale*, 2014, **6**, 2603-2607.
13. C. X. Guo, H. B. Yang, Z. M. Sheng, Z. S. Lu, Q. L. Song and C. M. Li, *Angew. Chem., Int. Ed.*, 2010, **49**, 3014-3017.
14. W. Song, X. Ji, W. Deng, Q. Chen, C. Shen and C. E. Banks, *Phys. Chem. Chem. Phys.*, 2013, **15**, 4799-4803.
15. A. B. Fuertes, F. Pico and J. M. Rojo, *J. Power Sources*, 2004, **133**, 329-336.
16. L. A. Ponomarenko, F. Schedin, M. I. Katsnelson, R. Yang, E. W. Hill, K. S. Novoselov and A. K. Geim, *Science*, 2008, **320**, 356-358.
17. D. Pan, J. Zhang, Z. Li and M. Wu, *Adv. Mater.*, 2010, **22**, 734-738.
18. J. Zhou, J. Cheiftz, R. Li, F. Wang, X. Zhou, T.-K. Sham, X. Sun and Z. Ding, *Carbon*, 2009, **47**, 829-838.
19. S. Zhuo, M. Shao and S.-T. Lee, *ACS Nano*, 2012, **6**, 1059-1064.
20. J. Lu, P. S. E. Yeo, C. K. Gan, P. Wu and K. P. Loh, *Nat Nano*, 2011, **6**, 247-252.
21. X. Yan, X. Cui and L.-s. Li, *J. Am. Chem. Soc.*, 2010, **132**, 5944-5945.
22. R. Liu, D. Wu, X. Feng and K. Müllen, *J. Am. Chem. Soc.*, 2011, **133**, 15221-15223.
23. W. S. Hummers and R. E. Offeman, *J. Am. Chem. Soc.*, 1958, **80**, 1339-1339.
24. C. E. Banks, T. J. Davies, G. G. Wildgoose and R. G. Compton, *Chem. Commun.*, 2005, DOI: 10.1039/B413177K, 829-841.
25. D. A. C. Brownson, L. J. Munro, D. K. Kampouris and C. E. Banks, *RSC Adv.*, 2011, **1**, 978-988.
26. K. Zhang, L. L. Zhang, X. S. Zhao and J. Wu, *Chem. Mater.*, 2010, **22**, 1392-1401.
27. Y. Zhu, S. Murali, M. D. Stoller, K. J. Ganesh, W. Cai, P. J. Ferreira, A. Pirkle, R. M. Wallace, K. A. Cychosz, M. Thommes, D. Su, E. A. Stach and R. S. Ruoff, *Science*, 2011, **332**, 1537-1541.
28. S. Murali, J. R. Potts, S. Stoller, J. Park, M. D. Stoller, L. L. Zhang, Y. Zhu and R. S. Ruoff, *Carbon*, 2012, **50**, 3482-3485.
29. K. S. Novoselov, A. K. Geim, S. V. Morozov, D. Jiang, Y. Zhang, S. V. Dubonos, I. V. Grigorieva and A. A. Firsov, *Science*, 2004, **306**, 666-669.
30. Y. Dong, C. Chen, X. Zheng, L. Gao, Z. Cui, H. Yang, C. Guo, Y. Chi and C. M. Li, *J. Mater. Chem.*, 2012, **22**, 8764-8766.
31. Y.-P. Sun, B. Zhou, Y. Lin, W. Wang, K. A. S. Fernando, P. Pathak, M. J. Meziani, B. A. Harruff, X. Wang, H. Wang, P. G. Luo, H. Yang, M. E. Kose, B. Chen, L. M. Veca and S.-Y. Xie, *J. Am. Chem. Soc.*, 2006, **128**, 7756-7757.
32. J. Zhou, C. Booker, R. Li, X. Zhou, T.-K. Sham, X. Sun and Z. Ding, *J. Am. Chem. Soc.*, 2007, **129**, 744-745.
33. A. Saha, S. K. Basiruddin, S. C. Ray, S. S. Roy and N. R. Jana, *Nanoscale*, 2010, **2**, 2777-2782.
34. X. Yang, X. Jia and X. Ji, *RSC Adv.*, 2015, **5**, 9337-9340.
35. I. Lavagnini, R. Antiochia and F. Magno, *Electroanalysis*, 2004, **16**, 505-506.
36. E. P. Randviir, D. A. C. Brownson, J. P. Metters, R. O. Kadara and C. E. Banks, *Phys. Chem. Chem. Phys.*, 2014, **16**, 4598-4611.
37. S. J. Konopka and B. McDuffie, *Anal. Chem.*, 1970, **42**, 1741-1746.
38. B. Šljukić, C. E. Banks and R. G. Compton, *Nano Lett.*, 2006, **6**, 1556-1558.
39. R. R. Moore, C. E. Banks and R. G. Compton, *Anal. Chem.*, 2004, **76**, 2677-2682.
40. A. Holloway, G. Wildgoose, R. Compton, L. Shao and M. H. Green, *J Solid State Electrochem*, 2008, **12**, 1337-1348.
41. J. Chmiola, C. Largeot, P.-L. Taberna, P. Simon and Y. Gogotsi, *Angew. Chem., Int. Ed.*, 2008, **47**, 3392-3395.
42. H. Hou, C. E. Banks, M. Jing, Y. Zhang and X. Ji, *Adv. Mater.*, 2015, DOI: 10.1002/adma.201503816, n/a-n/a.

We demonstrate that easy aggregation, rapid stacking and high oxygen-functional groups of GQDs have a negative impact on the electrochemical properties. GQDs are no better than graphene for an excellent single electrode material.